NeuroImage: Clinical 32 (2021) 102873

Contents lists available at ScienceDirect

NeuroImage: Clinical

journal homepage: www.elsevier.com/locate/ynicl

Locus coeruleus degeneration is associated with disorganized functional topology in Parkinson's disease

Cheng Zhou [a], Tao Guo [a], Xueqin Bai [a], JingJing Wu [a], Ting Gao [b], Xiaojun Guan [a], Xiaocao Liu [a], Luyan Gu [b], Peiyu Huang [a], Min Xuan [a], Quanquan Gu [a], Xiaojun Xu [a], Baorong Zhang [b], Minming Zhang [a,*]

[a] Department of Radiology, The Second Affiliated Hospital, Zhejiang University School of Medicine, 310000 Hangzhou, China
[b] Department of Neurology, The Second Affiliated Hospital, Zhejiang University School of Medicine, 310000 Hangzhou, China

ARTICLE INFO

Keywords:
Parkinson's disease
Locus coeruleus
Magnetic resonance imaging
Graph theory
Functional networks

ABSTRACT

Degeneration of the locus coeruleus (LC) is recognized as a critical hallmark of Parkinson's disease (PD). Recent studies have reported that noradrenaline produced from the LC has critical effects on brain functional organization. However, it is unknown if LC degeneration in PD contributes to cognitive/motor manifestations through modulating brain functional organization. This study enrolled 94 PD patients and 68 healthy controls, and LC integrity was measured using the contrast-to-noise ratio of the LC (CNR_{LC}) calculated from T1-weighted magnetic resonance imaging. We used graph-theory-based network analysis to characterize brain functional organization. The relationships among LC degeneration, network disruption, and cognitive/motor manifestations in PD were assessed. Whether network disruption was a mediator between LC degeneration and cognitive/motor impairments was assessed further. In addition, an independent PD subgroup (n = 35) having functional magnetic resonance scanning before and after levodopa administration was enrolled to evaluate whether LC degeneration-related network deficiencies were independent of dopamine deficiency. We demonstrated that PD patients have significant LC degeneration compared to healthy controls. CNR_{LC} was positively correlated with Montreal Cognitive Assessment score and the nodal efficiency (NE) of several cognitive-related regions. Lower NE of the superior temporal gyrus was a mediator between LC degeneration and cognitive impairment in PD. However, levodopa treatment could not normalize the reduced NE of the superior temporal gyrus (mediator). In conclusion, we provided evidence for the relationship between LC degeneration and extensive network disruption in PD, and highlight the role of network disorganization in LC degeneration-related cognitive impairment.

1. Introduction

Parkinson's disease (PD) is a common neurodegenerative disease characterized by degeneration of dopaminergic neurons in the substantia nigra (Kalia and Lang, 2015). In addition to this, studies have reported a 20%–90% loss of locus coeruleus (LC) cells in PD patients (Oertel et al., 2019; Giguère et al., 2018). The LC is the principal source of noradrenaline in the brain and is involved in cognitive and motor impairment in PD (Betts et al., 20192019; Espay et al., 2014). Over recent decades, a major emphasis has been placed on the symptom-related brain alterations caused by dopamine deficiency. How the brains of PD patients alter as a result of noradrenergic deficiency is largely unknown.

Dysregulation of the LC–noradrenaline system has been implicated

Abbreviations: **BC**, Betweenness centrality; **CG**, Cingulate gyrus; **CNR_{LC}**, Contrast-to-noise ratio of locus coeruleus; **Cun**, Cuneus; **DC**, Degree centrality; **FMG**, Middle frontal gyrus; **FuG**, Fusiform gyrus; **HC**, Healthy control; **H–Y**, Hoehn–Yahr stage; **IPL**, Inferior parietal lobule; **INS**, Insular gyrus; **LC**, Locus coeruleus; **LED**, Levodopa equivalent daily dose; **MoCA**, Montreal Cognitive Assessment; **NE**, Nodal efficiency; **OcG**, Occipital gyrus; **PD**, Parkinson's disease; **PCL**, Paracentral lobule; **PoG**, Postcentral gyrus; **PrG**, Precentral gyrus; **SFG**, Superior frontal gyrus; **STG**, Superior temporal gyrus; **UPDRS**, Unified Parkinson's Disease Rating Scale.

* Corresponding author.
E-mail addresses: 21718289@zju.edu.cn (C. Zhou), taoguo0331@zju.edu.cn (T. Guo), 11918449@zju.edu.cn (X. Bai), 21818300@zju.edu.cn (J. Wu), 11718327@zju.edu.cn (T. Gao), xiaojunguan1102@zju.edu.cn (X. Guan), 21918568@zju.edu.cn (X. Liu), 21918587@zju.edu.cn (L. Gu), hpyzju@foxmail.com (P. Huang), xuan_min@126.com (M. Xuan), zju_gqq@zju.edu.cn (Q. Gu), xxjmailbox@zju.edu.cn (X. Xu), brzhang@zju.edu.cn (B. Zhang), zhangminming@zju.edu.cn (M. Zhang).

https://doi.org/10.1016/j.nicl.2021.102873
Received 20 January 2021; Received in revised form 7 September 2021; Accepted 30 October 2021
Available online 3 November 2021

in numerous cognitive and behavioral symptoms of neurodegenerative diseases (Betts et al., 20192019; Gelbard-Sagiv et al., 2018; Kelberman et al., 2020). Research has suggested that the modulatory effects of the LC–noradrenaline system on behavior is closely linked with neuronal activity, consistent with the abundant projections from the noradrenergic neurons to other regions of the brain (Mather and Harley, 2016). This view has been confirmed both in mice models and humans: LC noradrenaline contributes to the reconfiguration of functional communication between brain regions (Gelbard-Sagiv et al., 2018; Zerbi et al., 2019). Pupil dilation, governed by noradrenergic and cholinergic systems, is also associated with brain functional connectivity (DiNuzzo et al., 2019; Mridha et al., 2021). Brain functional connectivity has been demonstrated to mediate the effect of a noradrenaline reuptake inhibitor on executive function in PD patients (Borchert et al., 2019). Whereas previous studies demonstrated the influence of the LC–noradrenaline system on cognitive performance, it is still largely unknown how LC degeneration in PD patients affects that system's interaction with other brain regions (Kelberman et al., 2020). It is of interest to explore the interaction between LC and other brain regions, and its connection with clinical manifestations further. Seed-based functional magnetic resonance imaging (fMRI) studies have reinforced the link between the LC and other brain regions, and its implications in cognitive processing (for a review, see (Liu et al., 2017). However; the small size of the LC and the low spatial resolution of fMRI limits our exploration (Liu et al., 2017).

The LC of humans can be visualized using magnetic resonance imaging (MRI) (Watanabe et al., 2019; Sasaki et al., 2008). The signal intensity calculated from T1-weighted MRI or magnetization transfer weighted MRI has been successfully used to evaluate the degeneration of LC neurons in vivo (Liu et al., 2017; Watanabe et al., 2019; Li et al., 2019; Chen et al., 2014). In this study, using recent methods, the contrast-to-noise ratio of the LC (CNR_{LC}) calculated from T1-weighted MRI was used to measure the integrity of the LC (Li et al., 2019; Wang et al., 2018). To characterize the functional organization of the brain, a widely used graph-theory-based network analysis was conducted. This approach was suitable to capture the complex functional alterations involving the interactions between multiple areas (Koshimori et al., 2016). Several local graph measures; including nodal degree centrality (DC), nodal betweenness centrality (BC), and nodal efficiency (NE), characterize the capacity and efficiency of information transfer, and are widely used in PD studies (Koshimori et al., 2016; Guan et al., 2019; Aracil-Bolaños et al., 2019). Effective functional organization of the brain is considered the foundation of cognitive and motor performance (Herrington et al., 2017; Hou et al., 2020; Gratton et al., 2019). Previous studies have strongly linked impaired functional organization in the temporal; prefrontal; and motor cortex to dysfunctional cognition and motor function in PD patients (Hou et al., 2020; Berman et al., 2016; Hou et al., 2018). Clarifying the complex relationships among LC degeneration; brain functional reorganization, and clinical manifestations might advance our knowledge of neuropathological changes in the LC, and might provide neuroimaging evidence for the importance of noradrenergic replacement therapy in PD patients (Oertel et al., 2019; Schindlbeck and Eidelberg, 2018).

Furthermore, the dopaminergic system has extensive neuron innervation and partly overlaps with the noradrenergic system (e.g., in the prefrontal cortex and sensorimotor cortex) (Benarroch, 2018). Numerous studies have reported the modulatory effect of levodopa on motor-related functional networks (Shine et al., 20192019; Akram, 2017; Shen et al., 2020). Therefore; clarifying whether LC degeneration-related network attributes are independent of dopamine deficiency might add to our knowledge on the impact that LC degeneration has on functional networks.

In summary, the aim of our study was to 1) assess the relationships between LC degeneration, brain network topology, and clinical manifestations in PD patients; 2) explore the potential mediating effect that network disruption in LC degeneration has on cognitive/motor impairments; and 3) clarify the effect that levodopa administration has on changes to LC degeneration-related networks.

2. Methods

2.1. Participants

This study was approved by the Medical Ethics Committee of the Second Affiliated Hospital of Zhejiang University School of Medicine. All participants signed informed consent forms in accordance with the Declaration of Helsinki. This study recruited 101 idiopathic PD patients from the Neurology Department of the Second Affiliated Hospital of Zhejiang University School of Medicine. PD was diagnosed by an experienced neurologist (B.Z.) according to the UK Parkinson's Disease Society Brain Bank diagnostic criteria (Hughes et al., 1992). For PD patients, clinical assessments and MRI scans were performed during OFF states (at least 12 h after withholding PD medication). Disease severity was assessed using the Unified Parkinson's Disease Rating Scale (UPDRS) and according to Hoehn–Yahr (H-Y) stage. Cognitive status was assessed using the Montreal Cognitive Assessment (MoCA) scale. Seventy-two HC individuals with an MoCA (Hong Kong version) score $>$ 22 were recruited from the community (Yeung et al., 2014). Subjects with a history of head injury, neurological surgery, intracranial mass, cerebrovascular disorders, or other neurological and psychiatric diseases, were excluded in this study. Participants with mean framewise displacement $>$0.2 mm during MRI scanning were also excluded. Therefore, we included 94 PD patients and 68 HC individuals in the final analysis.

Studies examining whether LC degeneration-related network attributes are modulated by levodopa are important. An independent PD subgroup that underwent UPDRS III assessment and fMRI scanning before and after levodopa administration was also enrolled in this study (Dirkx et al., 2019). Specifically, these evaluations were conducted during the OFF state and repeated 1 h after administration of 200 mg L-dopa and 50 mg benserazide (ON state). fMRI scans and clinical assessment during OFF and ON states were both conducted on the same morning. To rule out potential factors for levodopa resistance (e.g., gastro-intestinal malabsorption), (Dirkx et al., 2019) patients with greater than 20% improvement in UPDRS III score after levodopa administration were enrolled (n = 35). This group was termed the "PD_{sub}" group.

2.2. MRI scanning

All imaging data were acquired on a 3-tesla MRI scanner (Discovery MR750, GE Healthcare). The head of each participant was stabilized with foam pads. Earplugs were provided to reduce audible noise during scanning.

Three-dimensional T1-weighted (3D T1) images were acquired using a fast spoiled gradient-recalled sequence: echo time (TE) = 3.036 ms; repetition time (TR) = 7.336 ms; inversion time = 450 ms; flip angle (FA) = 11°; field of view (FOV) = 260 × 260 mm^2; matrix = 256 × 256; voxel size = 1 mm × 1 mm; slice thickness = 1.2 mm; number of slices = 196 (sagittal); scanning time = 5 min 53 s.

LC imaging was performed using a T1-weighted fast spin echo sequence: TE = 18.6 ms; TR = 600 ms; FA = 77°; FOV = 220 × 220 mm^2; matrix = 512 × 512; voxel size = 0.43 mm × 0.43 mm; slice thickness = 3 mm; slice gap = 0 mm; number of slices = 17 (axial). Scanning coverage was set from the top of basal ganglia to the bottom of the medulla oblongata; scanning time = 10 min 27 s.

Resting-state blood oxygen level-dependent MRI (rs-fMRI) data were acquired using a gradient-recalled echo–echo planar imaging sequence: TE = 30 ms; TR = 2000 ms; FA = 77°; FOV = 240 × 240 mm^2; voxel size = 3 mm × 3 mm; matrix = 64 × 64; slice thickness = 4 mm; slice gap = 0 mm; number of slices = 38 (axial); time points = 205; scanning time = 7 min.

2.3. CNR_{LC} calculation

An author (C.Z.), who was blinded to the subjects' information, performed two manual measurements with a time interval of one month. The intraclass correlation coefficient for the intra-rater agreement was 0.827. A radiology expert (Weiwen Zhou, also blinded to the subjects' information) was invited to perform one manual measurement. The intraclass correlation coefficient for the inter-rater agreement was 0.856. Manual measurements were processed using ITK-SNAP (https://sourceforge.net/projects/itk-snap/).

The LC was located in the bilateral areas of the dorsal pons symmetrically, adjacent to the fourth ventricle. Locations with highest signal intensity (SI) in three contiguous slices from the level of the inferior colliculi and extending to superior cerebellar peduncles were identified as LC. Circular regions of interest (ROIs) were demarcated in the bilateral LC and the mid-portions of the pons (PT) at the same slice (as a contrast area) (Li et al., 2019). The ROIs were placed at the predefined anatomical position of the LC if the signal was significantly reduced (one HC individual and five PD patients). As shown in Fig. 1, the size of the ROIs was 2 mm^2 for LC and 20 mm^2 for PT. The mean and standard deviation (SD) SI in bilateral LC and PT were calculated. The CNR_{LC} was calculated using the following equation: $CNR_{LC} = (SI_{LC} - SI_{PT}) / SD_{PT}$. Finally, the averaged CNR_{LC} value from three slices on right and left sides and three assessments were used for final analysis (Jiang et al., 2019).

2.4. fMRI data preprocessing

fMRI data preprocessing was performed using a MATLAB-based software package (https://github.com/weikanggong/Resting-state-fMRI-preprocessing) combining the FMRIB Software Library (FSL, https://fsl.fmrib.ox.ac.uk/fsl/fslwiki/), the BrainWavelet toolbox, (Patel et al., 2014) and Analysis of Functional NeuroImages (AFNI, https://afni.nimh.nih.gov/). The first 10 time points were excluded from the analysis to allow for scanner stabilization and the participants' adaptation to the environment. The remaining functional images were first corrected for within-scan differences in acquisition time between slices, followed by realignment to the middle volume to correct for interscan head motion. Participants with a mean framewise displacement >0.2 mm were excluded (Zhou et al., 2020). Subsequently, the processed images were registered to 3D T1 images and spatially normalized to a standard template (Montreal Neurological Institute). Corrected images were smoothed with a Gaussian kernel of 6 × 6 × 6 mm^3 and wavelet despiking was then conducted. Nuisance covariates, including white matter, cerebrospinal fluid, and 24 motion parameters, were regressed and temporal band-pass filtering (0.01–0.1 Hz) was applied.

2.5. Network construction

The node of brain network was defined using the human Brainnetome Atlas, which has 210 cortical and 36 subcortical regions (Fan et al., 2016). This is a cross-validated atlas containing information on functional and anatomical connections that is suitable for network analysis. The network correlation matrices for each subject were obtained by calculating the Pearson correlation coefficient between the mean time course of each pair of nodes. Accordingly, a 246 × 246 network correlation matrix was obtained for each subject. Fisher's Z-transformation

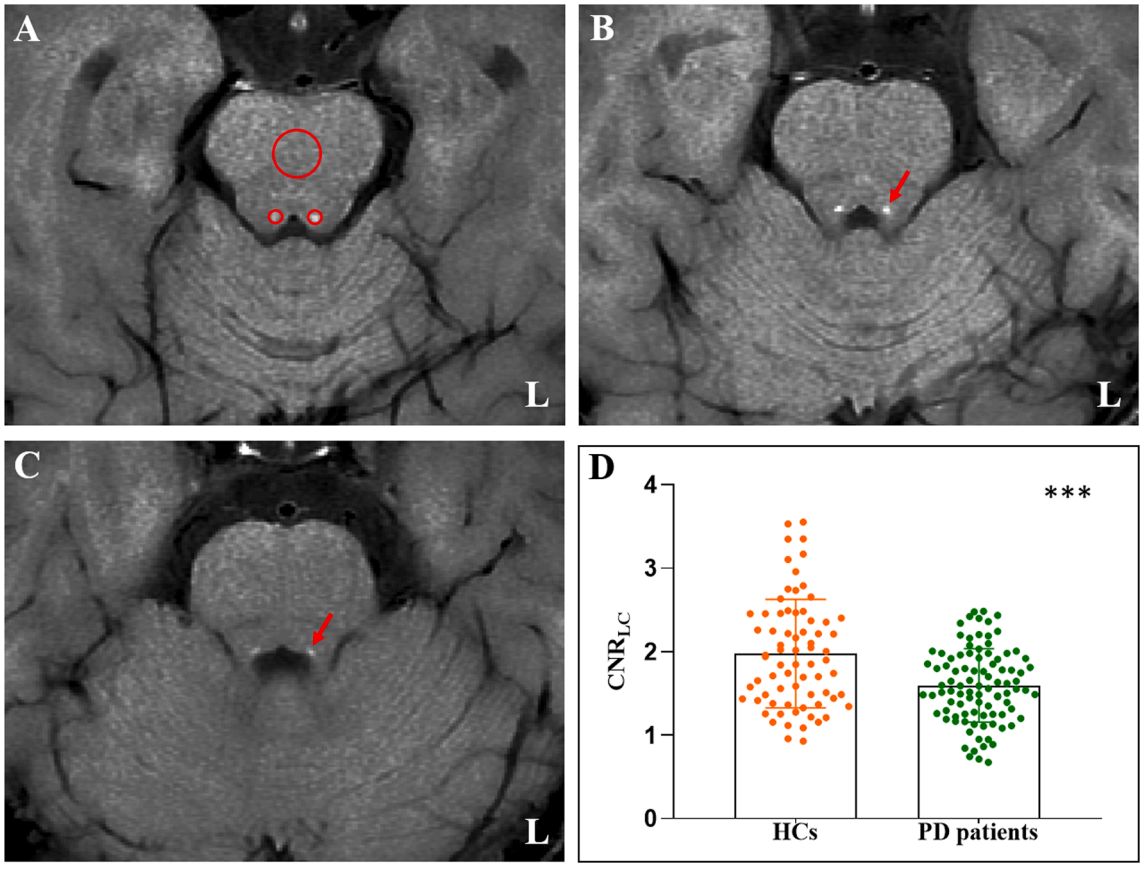

Fig. 1. Comparison of CNR_{LC} between the HC and PD groups. (A) Signal intensity measurements of the LC (two small red circles) and pons (a large red circles) from an HC individual. (B) and (C) The location of the LC in continuous layers (red arrow). (D) PD patients showed significant lower CNR_{LC} than the HC group. CNR_{LC}: Contrast-to-noise ratio of the locus coeruleus; HC: Healthy control; PD: Parkinson's disease; L: Left; ***: $p < 0.001$. (For interpretation of the references to colour in this figure legend, the reader is referred to the web version of this article.)

was applied for a graph theory-based network analysis.

2.6. Graph theory-based network analysis

Graph theory-based network analysis was conducted using the GRETNA toolbox (http://www.nitrc.org/projects/gretna/), (Wang et al., 2015) and the results were visualized using the BrainNet Viewer toolbox (http://www.nitrc.org/projects/bnv/) (Xia et al., 2013).

In the present study, nodal attributes, including nodal DC, nodal BC, and NE were used to determine nodal topological characteristics (Wang et al., 2015). DC represents the number of connections between one node and the others. A higher DC indicates greater significance of the node in the entire network and greater capacity for communicating information (Jiang et al., 2019). BC is defined as the number of shortest paths that go through a given node; a higher BC reflects a greater ability to link different parts of the network (Rubinov and Sporns, 2010). NE represents the ability of a given node to transmit information to the other nodes in the functional network; a higher NE indicates a greater ability to transfer information (Rubinov and Sporns, 2010).

Considering that network topological organization is significantly determined by network sparsity, we constructed 10 weighted connectivity matrices with different sparsity (5%–50% at 5% intervals) before calculating the network attributes. It is generally considered that constructed networks have prominent small-world properties in the range of 5%–50% (Watts and Strogatz, 1998). In line with previous studies; (Guan et al., 2019; Guan et al., 2019) we used the area under the curve (AUC)—a summarized indicator—of network attributes at 10 different sparsities to measure group differences and perform correlation analysis.

2.7. Statistical analysis

Statistical analysis was conducted using the Statistical Package for the Social Sciences (SPSS), version 22. Group comparisons of demographic and clinical data were assessed using the two-sample T-test or chi-squared test, as appropriate. CNR_{LC} and network attributes were analyzed using the general linear model (GLM) with age, gender, and education as covariates. Bonferroni correction was used for multiple comparisons of nodal attributes between HC and PD groups ($p < 0.05/246 = 0.0002$ was considered significant). Partial correlation analysis was performed for CNR_{LC}, damaged network attributes, and clinical variables (UPDRS III and MoCA) in the PD group. Age, gender, and education were used as covariates, and p values < 0.05 were considered significant.

Finally, mediation analysis was used to test whether LC degeneration-related clinical features can be explained by network disruption (the mediator). These analyses were performed using SPSS with 10,000 bootstraps. A standard three-variable path model was used. Age, gender, and education were used as covariates of no interest.

3. Results

3.1. Demographic, clinical and CNR_{LC} characteristics

The demographic, clinical, and CNR_{LC} characteristics are summarized in Table 1. No significant difference was found between the HC and PD groups in age and education. The two groups were statistically different in terms of gender, which was regressed out in the group comparison. The PD group showed significantly lower CNR_{LC} ($p < 0.001$; Fig. 1*D*) and MoCA score ($p = 0.001$; Table 1) than the HC group.

3.2. Group comparisons of network attributes between HC and PD

Compared with the HC group, the PD group had significantly lower DC of the superior frontal gyrus (SFG), middle frontal gyrus (FMG), precentral gyrus (PrG), postcentral gyrus (PoG), paracentral lobule (PCL), and cingulate gyrus (CG). Lower NE of vast regions, including the superior frontal gyrus (SFG), middle frontal gyrus (FMG), precentral gyrus (PrG), postcentral gyrus (PoG), paracentral lobule (PCL), inferior parietal lobule (IPL), cingulate gyrus (CG), superior temporal gyrus (STG), fusiform gyrus (FuG), insular gyrus (INS), cuneus (Cun), and occipital gyrus (OcG) were also found in the PD group (Fig. 2 and Supplementary Table 1). In addition, DC and NE of these regions were stably lower in the PD group under 10 different sparsities (Supplementary Fig. 1). No difference was found in BC between the PD and HC groups. Therefore, BC was excluded from further correlation analyses.

Table 1
Demographic and clinical characteristics.

	HC ($n = 68$)	PD ($n = 94$)	p value
Age	60.75 ± 7.41	60.64 ± 8.69	0.931
Gender (M/F)	29/39	57/37	0.024*
Education	8.24 ± 3.31	8.27 ± 4.38	0.952
Disease duration	–	3.92 ± 2.49	–
Duration of drug administration	–	2.94 ± 2.54	–
LED	–	435.00 ± 303.30	–
UPDRS I	–	1.34 ± 1.51	–
UPDRS II	–	6.82 ± 4.15	–
UPDRS III	–	17.23 ± 10.62	–
H-Y	–	2.05 ± 0.56	–
MoCA	24.86 ± 2.59	22.80 ± 5.21	0.001*
CNR_{LC}	1.97 ± 0.65	1.60 ± 0.44	<0.001*

HC: Healthy control; PD: Parkinson's disease; LED: Levodopa equivalent daily dose; UPDRS: Unified Parkinson's Disease Rating Scale; H-Y: Hoehn–Yahr; MoCA: Montreal Cognitive Assessment; CNR_{LC}: Contrast-to-noise ratio of the locus coeruleus.
Mean value and standard deviation were shown. $p < 0.05$ is considered as significant, and marked as *.

3.3. Relationships between the CNR_{LC}, nodal attributes, and clinical data in PD patients

In the PD group, the CNR_{LC} was positively correlated with the MoCA score ($R = 0.215$, $p = 0.041$; Fig. 3*A*). The CNR_{LC} was positively associated with the NE of several cognitive-related regions (Fig. 3*B*) including the right STG ($R = 0.292$, $p = 0.005$), right INS ($R = 0.259$, $p = 0.013$), right Cun ($R = 0.276$, $p = 0.008$), and left Cun ($R = 0.274$, $p = 0.009$). We also observed significant positive correlations between the CNR_{LC} and the NE of the sensorimotor cortex, including the left PrG ($R = 0.299$, $p = 0.004$) and left PoG ($R = 0.229$, $p = 0.013$; Fig. 3*B*). The p values were not significant after Bonferroni correction, but remained significant after false discovery rate correction.

In addition, the NE of the right STG ($R = 0.287$, $p = 0.006$) and right INS ($R = 0.234$, $p = 0.026$) were significantly correlated with MoCA score (Fig. 3*C*). Therefore, we conducted a mediation analysis to test whether the NEs of the right STG and right INS were statistical mediators between LC degeneration and cognitive decline. Mediation analysis with 10,000 bootstraps demonstrated that the relationship between CNR_{LC} and MoCA is totally mediated by the NE of STG (Fig. 3*D*).

3.4. The specificity of network disruption associated with LC degeneration

The PD_{sub} group ($n = 35$) showed no significant difference in age, gender, and education when compared with HC ($n = 68$) and PD groups ($n = 94$). Compared with the HC group, the PD_{sub} group showed a lower MoCA score ($p = 0.047$). No significant difference was found in disease duration, duration of drug administration, levodopa equivalent daily dose, and UPDRS I, UPDRS II, UPDRS III, H-Y and MoCA scores between two the PD groups (Supplementary Table 2).

The PD_{sub} group showed significantly lower nodal attributes in the above regions than the HC group (Supplementary Table 3). These results were highly consistent with the comparison between HC and PD groups. There was no difference in the above nodal attributes between PD_{sub} and PD groups (Supplementary Table 3), which indicated a high

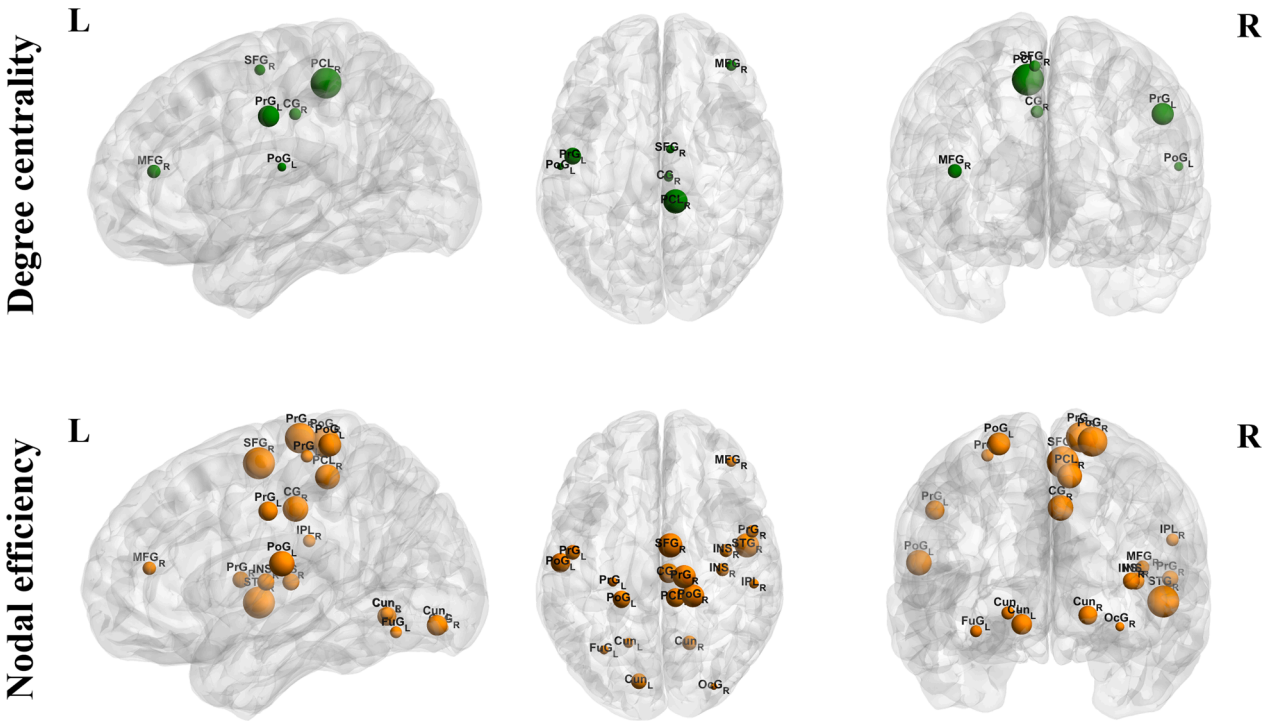

Fig. 2. Differences of network attributes between HC and PD groups. HC: Healthy control; PD: Parkinson's disease; DC: Degree centrality; NE: Nodal efficiency; L: Left; R: Right; SFG: Superior frontal gyrus; PoG: Postcentral gyrus; CG: Cingulate gyrus; FMG: Middle frontal gyrus; PrG: Precentral gyrus; PCL: Paracentral lobule; FuG: Fusiform gyrus; IPL: Inferior parietal lobule; PoG: Postcentral gyrus; INS: Insular gyrus; Cun: Cuneus; OcG: Occipital gyrus; STG: Superior temporal gyrus. Green/orange means HC > PD. (For interpretation of the references to colour in this figure legend, the reader is referred to the web version of this article.)

homogeneity between the two groups. The PD_{sub} group showed significantly higher DC of the right SFG ($p = 0.022$) and left PrG ($p = 0.046$), and NE of the right SFG ($p = 0.044$). These regions are located in the frontal and sensorimotor cortex, which are considered dopaminergic innervated brain regions (Akram, 2017). However; the NE of STG (mediator) showed no increase after levodopa administration, indicating that the mediator was specific for LC noradrenaline, and independent of dopamine ($p = 0.096$; Supplementary Table 3).

4. Discussion

This study investigated the relationships among LC degeneration, network disruption, and cognitive impairment in a large sample of PD patients. We confirmed the relationship between LC degeneration and cognitive impairment in PD patients, which had been reported by a recent study with moderate sample size (Prasuhn et al., 2021). We further highlight the role of network disorganization in LC degeneration-related cognitive impairment.

4.1. LC degeneration and cognitive impairment in PD patients

Braak and Del Tredici confirmed that the LC is degenerated at the early stages of PD owing to the Lewy pathology (Braak and Del Tredici, 2017). In line with previous studies; (Ohtsuka et al., 2013; Kitao et al., 2013) we detected significant LC degeneration in PD patients. Moreover; we found that LC degeneration was associated with cognitive decline in our PD group. The relationship between LC and cognition have been described in previous cognitive neuroscience studies (Clewett et al., 2018; Clewett et al., 2016; Clewett, 2019). In PD studies; previous study reported that PD dementia was associated with the loss of noradrenergic neurons in the LC; (Del Tredici and Braak, 2013) pharmacological research shows that inhibiting noradrenergic neurotransmission reduced cognitive performance of PD patients (Cash et al., 1987). Consistent with that, recent MRI studies demonstrated the relationship between LC degeneration and cognitive impairment in PD patients (Li et al., 2019; Prasuhn et al., 2021). The present study confirms the relationship between LC degeneration and cognitive impairment in a large sample size of PD patients; and suggests that therapies targeted to the noradrenergic system might be clinically significant (Feinstein et al., 2016).

4.2. LC integrity is associated with network disruption in the cognitive-related cortex

Significantly decreased nodal attributes were found in extensive cortical regions, which means that PD patients have less connectivity and lower efficiency of information transmission (Hillary and Grafman, 2017; Fang et al., 2017). These results further confirmed and extended existing knowledge on widespread functional disorganization (Knudsen et al., 2018).

In this study, we demonstrated that decreased LC integrity was significantly associated with the lower efficiency of the cognitive-related cortex, including the STG, INS, and Cun. Lower NEs of STG and INS were correlated with worse cognitive performance. It is known that the LC–noradrenaline system projects into multiple cortical domains (Bari et al., 2020). Previous studies have shown that LC activation induced increases in the connectivity of temporal and insular gyri (Zerbi et al., 2019; Bouret, 2019). Postmortem studies have confirmed that a deficiency of LC noradrenaline was most prominent in the temporal lobe of Alzheimer's disease patients (Nazarali and Reynolds, 1992). The visuospatial function-related cuneus also has abundant functional connectivity to the LC (Zhang et al., 2016). Therefore; these findings highlight the importance of LC integrity on the topological organization of the cognitive-related cortex.

Furthermore, we found that reduced NE of the right STG was a mediator between decreased LC integrity and cognitive impairment in PD patients. Also, levodopa replacement therapy could not improve the NE of the right STG. Similarly, two studies have reported the modulatory

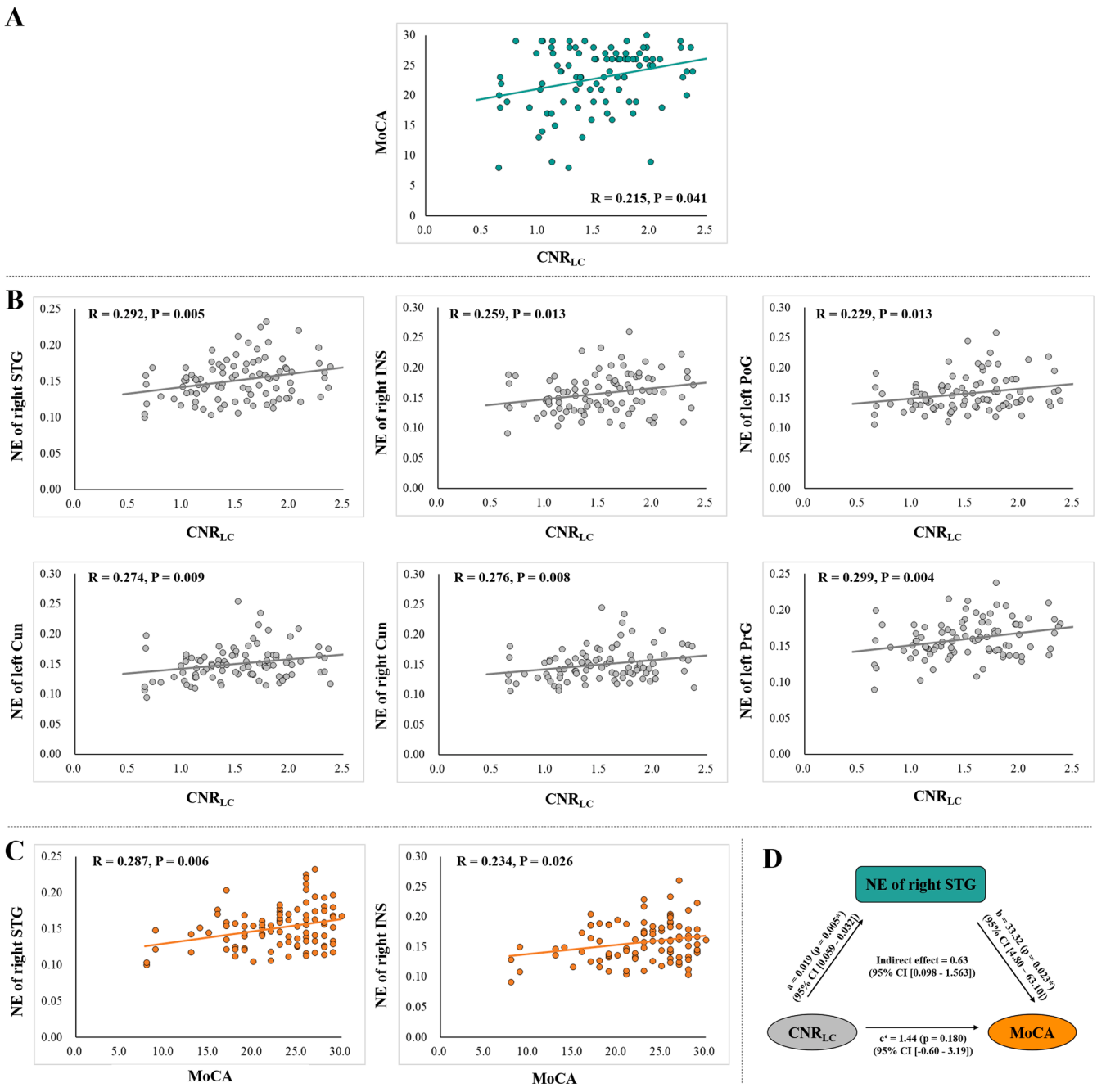

Fig. 3. Correlation analysis among CNR_{LC}, network attributes, and MoCA score in PD group. (A) CNR_{LC} was significantly correlated with MoCA score in the PD group. (B) CNR_{LC} was significantly correlated with the network attributes of cognitive- and motor-related regions in the PD group. (C) Network attributes of two cognitive-related regions were associated with MoCA score in the PD group. (D) Mediation analysis showed that reduced NE of the STG was a mediator between LC degeneration and cognitive decline. CNR_{LC}: Contrast-to-noise ratio of the locus coeruleus; MoCA: Montreal Cognitive Assessment; PD: Parkinson's disease; DC: Degree centrality; NE: Nodal efficiency; STG: Superior temporal gyrus; INS: Insular gyrus; IPL: Inferior parietal lobule; Cun: Cuneus; PrG: Precentral gyrus.

effect of atomoxetine, a selective noradrenaline reuptake inhibitor, on functional network organization (both left and right STG were involved) in PD patients (Borchert et al., 2019; Rae et al., 2016). Although we only demonstrated a mediating effect in the right side; future study should further confirm whether there is lateralization in the mediating effect. Our previous study also demonstrated that temporal atrophy plays a key role in the process of cognitive deterioration in PD (Zhou et al., 2020).

Finally, we demonstrated that the NE of the STG could not be modulated by levodopa administration. This finding further suggested that the linking among LC integrity, STG disorganization, and cognitive impairment might be independent of the dopaminergic system. This finding was also supported by one of the latest studies, which suggested that SN degeneration correlates with motor dysfunction, whereas LC degeneration is related to cognitive impairment in PD patients (Prasuhn et al., 2021). However, it is worth noting that confidence in the negative result (levodopa challenge test) might be less because of the small sample size of that study. Other neurotransmitter systems (e.g., serotonergic, cholinergic) might be involved in cognition-related pathways (O'Callaghan and Lewis, 2017). Investigating the effects of interactions among dopaminergic; noradrenergic, serotonergic, and cholinergic systems in a large sample of PD patients would be a significant development.

Our findings imply that LC degeneration may contributes to functional disorganization, which in turn causes cognitive impairment in PD

patients. These findings extend our knowledge about the modulatory effect of the noradrenergic system in cognitive impairment in PD. Compared with the irreversible degeneration of the LC, functional network attributes might be effective indicators for monitoring the response of noradrenergic therapies.

4.3. LC degeneration associated with network disruption in the sensorimotor cortex

We also demonstrated a significant positive association between LC integrity and the NE of the sensorimotor cortex, including PrG and PoG. The sensorimotor cortex receives abundant innervation from LC noradrenergic neurons (Benarroch, 2018). It is reasonable to suggest that LC degeneration contributes to sensorimotor cortex disorganization. However; no direct correlation was found between LC degeneration and motor performance (UPDRS III score). Although no significant linear correlation was found between LC degeneration and UPDRS III, experimental evidence from animal studies has suggested that LC neuron loss enhances neurodegeneration of the nigrostriatal dopaminergic system and aggravates motor disturbance (Fornai et al., 1996; Ferrucci et al., 2002). On account of the complex innervation of the sensorimotor cortex, we assumed that there is an interaction between the dopaminergic and noradrenergic systems in the sensorimotor cortex (Sara, 2009). This assumption was partly supported by our findings: reduced nodal attributes of the sensorimotor cortex could be normalized by levodopa; which implies that the dopaminergic system is also linked with the sensorimotor cortex. A previous study also suggested that dopaminergic deficiency contributes to disorganization of the sensorimotor cortex, and that administration of levodopa can normalize it (Akram, 2017).

Nevertheless, the negative findings between LC integrity and motor dysfunction do not mean that they are independent. We demonstrated a significant relationship between LC degeneration and functional organization of the motor cortex. In addition, we demonstrated a significant relationship between LC degeneration and motor response to levodopa in recent published paper (Zhou et al., 2021). Therefore; the interactions between the dopaminergic and noradrenergic systems require further investigation.

5. Limitations

One of the limitations of our study is the small size of the PD_{sub} group receiving levodopa administration. It would be useful to validate the current findings at a higher resolution and using isotropic LC imaging, because a slice thickness of 3 mm, as used in our study, is susceptible to partial volume effects (Priovoulos et al., 2018). In addition, a recent study suggested that the high signal intensity in the LC was largely attributable to the density of intracellular water protons but not the neuromelanin (Watanabe et al., 2019). Although the signal intensity was useful in evaluating the integrity of the LC; (Watanabe et al., 2019) it is important to confirm the present findings using more direct methods (e.g., positron emission tomography, measures of noradrenergic transporter levels). In this study, the CNR_{LC} have no age-relationship, which is inconsistent with previous study (Clewett et al., 2016). This may impact the correlation analysis in which age is included as covariate. Therefore; the relationship between LC and cognition should be interpreted cautiously. It should also be noted that the correlations between CNR_{LC} and network attributes did not hold after strict Bonferroni correction. This indicates that the power might be relatively low, and future studies utilizing LC imaging with higher resolution or positron emission tomography for confirming the relationship between LC degeneration and network organization will be meaningful. Gender was not perfectly matched in the PD and HC groups, although we included it as a covariate in the statistical analysis. Finally, the relationship between LC degeneration and cognitive impairment in different domains should be assessed in the future.

In conclusion, this study provided evidence for the relationship between LC degeneration and extensive network disruption in PD patients. And the network disorganization may play an important role of in LC degeneration-related cognitive impairment. These findings highlight the necessity of an adjuvant therapy that targets the noradrenergic system, and that functional organization might be a potential indicator for monitoring the response of noradrenergic therapies.

CRediT authorship contribution statement

Cheng Zhou: Conceptualization, Formal analysis, Methodology, Writing – review & editing, Visualization. **Tao Guo:** Formal analysis, Methodology, Writing – review & editing, Resources. **Xueqin Bai:** Formal analysis, Methodology, Writing – review & editing, Resources. **JingJing Wu:** Resources, Resources, Visualization. **Ting Gao:** Resources, Resources, Visualization. **Xiaojun Guan:** Resources, Writing – review & editing. **Xiaocao Liu:** Resources. **Luyan Gu:** Resources. **Peiyu Huang:** Data curation, Writing – review & editing. **Min Xuan:** Writing – review & editing. **Quanquan Gu:** Writing – review & editing. **Xiaojun Xu:** Funding acquisition, Supervision. **Baorong Zhang:** Conceptualization, Supervision, Writing – review & editing. **Minming Zhang:** Conceptualization, Data curation, Funding acquisition, Project administration, Supervision, Writing – review & editing.

Declaration of Competing Interest

The authors declare that they have no known competing financial interests or personal relationships that could have appeared to influence the work reported in this paper.

Acknowledgements

We thank Weiwen Zhou for her professional work in ROI drawing, and all the participants that enrolled in this study.

Study funding

This work was supported by the 13th Five-year Plan for National Key Research and Development Program of China (Grant No. 2016YFC1306600), the National Natural Science Foundation of China (Grant Nos. 82171888, 82001767, 81971577, and 82001353), the Natural Science Foundation of Zhejiang Province (Grant No. LQ21H180008 and LQ20H180012), the China Postdoctoral Science Foundation (Grant Nos. 2021T140599 and 2019M662082), the National Natural Science Foundation of China's Major Regional International Cooperation Project (Grant No. 81520108010), and the Key Research and Development Program of Zhejiang Province (Grant No. 2020C03020).

Data availability

The datasets generated and/or analyzed during this study are available from the corresponding author upon reasonable request.

Disclosure

The authors report no disclosures relevant to the manuscript.

Appendix A. Supplementary data

Supplementary data to this article can be found online at https://doi.org/10.1016/j.nicl.2021.102873.

References

Akram, H., et al., 2017. l-Dopa responsiveness is associated with distinctive connectivity patterns in advanced Parkinson's disease. Movement Disord. 32, 874–883. https://doi.org/10.1002/mds.27017.

Aracil-Bolaños, I., Sampedro, F., Marín-Lahoz, J., Horta-Barba, A., Martínez-Horta, S., Botí, M., Pérez-Pérez, J., Bejr-Kasem, H., Pascual-Sedano, B., Campolongo, A., Izquierdo, C., Gironell, A., Gómez-Ansón, B., Kulisevsky, J., Pagonabarraga, J., 2019. A divergent breakdown of neurocognitive networks in Parkinson's Disease mild cognitive impairment. Hum. Brain Mapp. 40 (11), 3233–3242.

Bari, B., Chokshi, V., Schmidt, K., 2020. Locus coeruleus-norepinephrine: basic functions and insights into Parkinson's disease. Neural Regener. Res. 15 (6), 1006. https://doi.org/10.4103/1673-5374.270297.

Benarroch, E.E., 2018. Locus coeruleus. Cell Tissue Res. 373 (1), 221–232. https://doi.org/10.1007/s00441-017-2649-1.

Berman, B.D., Smucny, J., Wylie, K.P., Shelton, E., Kronberg, E., Leehey, M., Tregellas, J. R., 2016. Levodopa modulates small-world architecture of functional brain networks in Parkinson's disease. Mov. Disord. 31 (11), 1676–1684. https://doi.org/10.1002/mds.26713.

Betts, M. J. *et al.* Locus coeruleus imaging as a biomarker for noradrenergic dysfunction in neurodegenerative diseases. *Brain* **142**, 2558-2571, doi:10.1093/brain/awz193 (2019).

Borchert, R. J. *et al.* Atomoxetine and citalopram alter brain network organization in Parkinson's disease. *Brain Commun.* **1**, fcz013, doi:10.1093/braincomms/fcz013 (2019).

Bouret, S., 2019. Locus coeruleus, noradrenaline, and behavior: network effect, network effects? Neuron 103 (4), 554–556. https://doi.org/10.1016/j.neuron.2019.07.033.

Braak, H., Del Tredici, K., 2017. Neuropathological staging of brain pathology in sporadic Parkinson's disease: separating the wheat from the chaff. J. Parkinson's Dis. 7 (s1), S71–S85. https://doi.org/10.3233/JPD-179001.

Cash, R. *et al.* Parkinson's disease and dementia: norepinephrine and dopamine in locus ceruleus. *Neurology* **37**, 42-46, doi:10.1212/wnl.37.1.42 (1987).

Chen, X., Huddleston, D.E., Langley, J., Ahn, S., Barnum, C.J., Factor, S.A., Levey, A.I., Hu, X., 2014. Simultaneous imaging of locus coeruleus and substantia nigra with a quantitative neuromelanin MRI approach. Magn. Reson. Imaging 32 (10), 1301–1306. https://doi.org/10.1016/j.mri.2014.07.003.

Clewett, D. V., Huang, R. Locus Coeruleus activity strengthens prioritized memories under arousal. **38**, 1558–1574, doi:10.1523/jneurosci.2097-17.2017 (2018).

Clewett, D.V., Lee, T.-H., Greening, S., Ponzio, A., Margalit, E., Mather, M., 2016. Neuromelanin marks the spot: identifying a locus coeruleus biomarker of cognitive reserve in healthy aging. Neurobiol Aging 37, 117–126. https://doi.org/10.1016/j.neurobiolaging.2015.09.019.

Clewett, D., Murty, V.P., 2019. Echoes of emotions past: how neuromodulators determine what we recollect. **6**, doi:10.1523/eneuro.0108-18.2019.

Del Tredici, K., Braak, H., 2013. Dysfunction of the locus coeruleus-norepinephrine system and related circuitry in Parkinson's disease-related dementia. J. Neurol. Neurosurg. Psychiatry 84 (7), 774–783. https://doi.org/10.1136/jnnp-2011-301817.

DiNuzzo, M., Mascali, D., Moraschi, M., Bussu, G., Maugeri, L., Mangini, F., Fratini, M., Giove, F., 2019. Brain networks underlying eye's pupil dynamics. Front. Neurosci. 13 https://doi.org/10.3389/fnins.2019.00965.

Dirkx, M. F. *et al.* Cerebral differences between dopamine-resistant and dopamine-responsive Parkinson's tremor. *Brain* **142**, 3144–3157, doi:10.1093/brain/awz261 (2019).

Espay, A.J., LeWitt, P.A., Kaufmann, H., 2014. Norepinephrine deficiency in Parkinson's disease: the case for noradrenergic enhancement. Movem. Disord. 29 (14), 1710–1719. https://doi.org/10.1002/mds.v29.1410.1002/mds.26048.

Fan, L., Li, H., Zhuo, J., Zhang, Y.u., Wang, J., Chen, L., Yang, Z., Chu, C., Xie, S., Laird, A.R., Fox, P.T., Eickhoff, S.B., Yu, C., Jiang, T., 2016. The Human Brainnetome Atlas: a new brain atlas based on connectional architecture. Cereb. Cortex 26 (8), 3508–3526. https://doi.org/10.1093/cercor/bhw157.

Fang, J., Chen, H., Cao, Z., Jiang, Y., Ma, L., Ma, H., Feng, T., 2017. Impaired brain network architecture in newly diagnosed Parkinson's disease based on graph theoretical analysis. Neurosci. Lett. 657, 151–158. https://doi.org/10.1016/j.neulet.2017.08.002.

Feinstein, D.L., Kalinin, S., Braun, D., 2016. Causes, consequences, and cures for neuroinflammation mediated via the locus coeruleus: noradrenergic signaling system. J. Neurochem. 139 (Suppl 2), 154–178. https://doi.org/10.1111/jnc.13447.

Ferrucci, M., Gesi, M., Lenzi, P., Soldani, P., Ruffoli, R., Pellegrini, A., Ruggieri, S., Paparelli, A., Fornai, F., 2002. Noradrenergic loss enhances MDMA toxicity and induces ubiquitin-positive striatal whorls. Neurol. Sci. 23 (0), s75–s76. https://doi.org/10.1007/s100720200077.

Fornai, F., Torracca, M.T., Bassi, L., D'Errigo, D.A., Scalori, V., Corsini, G.U., 1996. Norepinephrine loss selectively enhances chronic nigrostriatal dopamine depletion in mice and rats. Brain Res 735 (2), 349–353. https://doi.org/10.1016/0006-8993(96)00891-8.

Gelbard-Sagiv, H., Magidov, E., Sharon, H., Hendler, T. & Nir, Y. Noradrenaline modulates visual perception and late visually evoked activity. *Curr. Boil.: CB* **28**, 2239-2249 e2236, doi:10.1016/j.cub.2018.05.051 (2018).

Giguère, N., Burke Nanni, S., Trudeau, L.-E. On cell loss and selective vulnerability of neuronal populations in Parkinson's disease. *Front. Neurol.* **9**, doi:10.3389/fneur.2018.00455 (2018).

Gratton, C. *et al.* Emergent functional network effects in Parkinson disease. *Cerebral cortex (New York, N.Y. : 1991)* **29**, 2509-2523, doi:10.1093/cercor/bhy121 (2019).

Guan, X., Guo, T., Zeng, Q., Wang, J., Zhou, C., Liu, C., Wei, H., Zhang, Y., Xuan, M., Gu, Q., Xu, X., Huang, P., Pu, J., Zhang, B., Zhang, M.-M., 2019. Oscillation-specific nodal alterations in early to middle stages Parkinson's disease. Translational Neurodegener. 8 (1).

Guan, X., Zhang, Y., Wei, H., Guo, T., Zeng, Q., Zhou, C., Wang, J., Gao, T., Xuan, M., Gu, Q., Xu, X., Huang, P., Pu, J., Zhang, B., Liu, C., Zhang, M., 2019. Iron-related nigral degeneration influences functional topology mediated by striatal dysfunction in Parkinson's disease. Neurobiol Aging 75, 83–97. https://doi.org/10.1016/j.neurobiolaging.2018.11.013.

Herrington, T.M., Briscoe, J., Eskandar, E., 2017. Structural and functional network dysfunction in Parkinson disease. Radiology 285 (3), 725–727. https://doi.org/10.1148/radiol.247172401.

Hillary, F.G., Grafman, J.H., 2017. Injured brains and adaptive networks: the benefits and costs of hyperconnectivity. Trends Cognitive Sci. 21 (5), 385–401. https://doi.org/10.1016/j.tics.2017.03.003.

Hou, Y., Wei, Q., Ou, R., Yang, J., Song, W., Gong, Q., Shang, H., 2018. Impaired topographic organization in cognitively unimpaired drug-naïve patients with rigidity-dominant Parkinson's disease. Parkinsonism Relat. Disord. 56, 52–57. https://doi.org/10.1016/j.parkreldis.2018.06.021.

Hou, Y., Wei, Q., Ou, R., Yang, J., Gong, Q., Shang, H., 2020. Impaired topographic organization in Parkinson's disease with mild cognitive impairment. J. Neurol. Sci. 414, 116861. https://doi.org/10.1016/j.jns.2020.116861.

Hughes, A.J., Daniel, S.E., Kilford, L., Lees, A.J., 1992. Accuracy of clinical diagnosis of idiopathic Parkinson's disease: a clinico-pathological study of 100 cases. J. Neurol. Neurosurg. Psychiatry 55 (3), 181–184. https://doi.org/10.1136/jnnp.55.3.181.

Jiang, W., Lei, Y., Wei, J., Yang, L.u., Wei, S., Yin, Q., Luo, S., Guo, W., 2019. Alterations of interhemispheric functional connectivity and degree centrality in cervical dystonia: a resting-state fMRI Study. Neural Plasticity 2019, 1–11. https://doi.org/10.1155/2019/7349894.

Kalia, L.V., Lang, A.E., 2015. Parkinson's disease. Lancet (London, England) 386 (9996), 896–912. https://doi.org/10.1016/S0140-6736(14)61393-3.

Kelberman, M., Keilholz, S., Weinshenker, D., 2020. What's that (Blue) spot on my MRI? multimodal neuroimaging of the locus coeruleus in neurodegenerative disease. Front. Neurosci. 14, 583421 https://doi.org/10.3389/fnins.2020.583421.

Kitao, S., Matsusue, E., Fujii, S., Miyoshi, F., Kaminou, T., Kato, S., Ito, H., Ogawa, T., 2013. Correlation between pathology and neuromelanin MR imaging in Parkinson's disease and dementia with Lewy bodies. Neuroradiology 55 (8), 947–953. https://doi.org/10.1007/s00234-013-1199-9.

Knudsen, K., Fedorova, T.D., Hansen, A.K., Sommerauer, M., Otto, M., Svendsen, K.B., Nahimi, A., Stokholm, M.G., Pavese, N., Beier, C.P., Brooks, D.J., Borghammer, P., 2018. In-vivo staging of pathology in REM sleep behaviour disorder: a multimodality imaging case-control study. Lancet Neurol. 17 (7), 618–628. https://doi.org/10.1016/S1474-4422(18)30162-5.

Koshimori, Y., Cho, S.-S., Criaud, M., Christopher, L., Jacobs, M., Ghadery, C., Coakeley, S., Harris, M., Mizrahi, R., Hamani, C., Lang, A.E., Houle, S., Strafella, A. P., 2016. Disrupted nodal and hub organization account for brain network abnormalities in Parkinson's disease. Front. Aging Neurosci. 8.

Li, Y., Wang, C., Wang, J., Zhou, Y., Ye, F., Zhang, Y., Cheng, X., Huang, Z., Liu, K., Fei, G., Zhong, C., Zeng, M., Jin, L., 2019. Mild cognitive impairment in de novo Parkinson's disease: a neuromelanin MRI study in locus coeruleus. Movement Disord. 34 (6), 884–892. https://doi.org/10.1002/mds.v34.610.1002/mds.27682.

Liu, K.Y., Marijatta, F., Hämmerer, D., Acosta-Cabronero, J., Düzel, E., Howard, R.J., 2017. Magnetic resonance imaging of the human locus coeruleus: a systematic review. Neurosci. Biobehav. Rev. 83, 325–355. https://doi.org/10.1016/j.neubiorev.2017.10.023.

Mather, M., Harley, C.W., 2016. The locus coeruleus: essential for maintaining cognitive function and the aging brain. Trends Cognitive Sci. 20 (3), 214–226. https://doi.org/10.1016/j.tics.2016.01.001.

Mridha, Z., de Gee, J. W. Graded recruitment of pupil-linked neuromodulation by parametric stimulation of the vagus nerve. **12**, 1539, doi:10.1038/s41467-021-21730-2 (2021).

Nazarali, A.J., Reynolds, G.P., 1992. Monoamine neurotransmitters and their metabolites in brain regions in Alzheimer's disease: a postmortem study. Cell. Mol. Neurobiol. 12 (6), 581–587. https://doi.org/10.1007/BF00711237.

O'Callaghan, C., Lewis, S.J.G., 2017. Cognition in Parkinson's Disease. Int. Rev. Neurobiol. 133, 557–583. https://doi.org/10.1016/bs.irn.2017.05.002.

Oertel, W.H., Henrich, M.T., Janzen, A., Geibl, F.F., 2019. The locus coeruleus: Another vulnerability target in Parkinson's disease. Movem. Dis. 34 (10), 1423–1429. https://doi.org/10.1002/mds.v34.1010.1002/mds.27785.

Ohtsuka, C., Sasaki, M., Konno, K., Koide, M., Kato, K., Takahashi, J., Takahashi, S., Kudo, K., Yamashita, F., Terayama, Y., 2013. Changes in substantia nigra and locus coeruleus in patients with early-stage Parkinson's disease using neuromelanin-sensitive MR imaging. Neurosci. Lett. 541, 93–98. https://doi.org/10.1016/j.neulet.2013.02.012.

Patel, A.X., Kundu, P., Rubinov, M., Jones, P.S., Vértes, P.E., Ersche, K.D., Suckling, J., Bullmore, E.T., 2014. A wavelet method for modeling and despiking motion artifacts from resting-state fMRI time series. Neuroimage 95, 287–304. https://doi.org/10.1016/j.neuroimage.2014.03.012.

Prasuhn, J., Prasuhn, M. Association of Locus Coeruleus and Substantia Nigra Pathology With Cognitive and Motor Functions in Patients With Parkinson Disease. (2021).

Prasuhn, J., Prasuhn, M., Fellbrich, A., Strautz, R., Lemmer, F., Dreischmeier, S., Kasten, M., Münte, T.F., Hanssen, H., Heldmann, M., Brüggemann, N., 2021. Association of Locus Coeruleus and Substantia Nigra pathology with cognitive and motor functions in patients with Parkinson disease. Neurology 97 (10), e1007–e1016. https://doi.org/10.1212/WNL.0000000000012444.

Priovoulos, N., Jacobs, H.I.L., Ivanov, D., Uludağ, K., Verhey, F.R.J., Poser, B.A., 2018. High-resolution in vivo imaging of human locus coeruleus by magnetization transfer

MRI at 3T and 7T. Neuroimage 168, 427–436. https://doi.org/10.1016/j.neuroimage.2017.07.045.
Rae, C.L., Nombela, C., Rodríguez, P.V., Ye, Z., Hughes, L.E., Jones, P.S., Ham, T., Rittman, T., Coyle-Gilchrist, I., Regenthal, R., Sahakian, B.J., Barker, R.A., Robbins, T.W., Rowe, J.B., 2016. Atomoxetine restores the response inhibition network in Parkinson's disease. Brain 139 (8), 2235–2248. https://doi.org/10.1093/brain/aww138.
Rubinov, M., Sporns, O., 2010. Complex network measures of brain connectivity: uses and interpretations. Neuroimage 52 (3), 1059–1069. https://doi.org/10.1016/j.neuroimage.2009.10.003.
Sara, S.J., 2009. The locus coeruleus and noradrenergic modulation of cognition. Nat. Rev. Neurosci. 10 (3), 211–223. https://doi.org/10.1038/nrn2573.
Sasaki, M. *et al.* Monoamine neurons in the human brain stem: anatomy, magnetic resonance imaging findings, and clinical implications. *Neuroreport* **19**, 1649-1654, doi:10.1097/WNR.0b013e328315a637 (2008).
Schindlbeck, K.A., Eidelberg, D., 2018. Network imaging biomarkers: insights and clinical applications in Parkinson's disease. Lancet. Neurology 17 (7), 629–640. https://doi.org/10.1016/S1474-4422(18)30169-8.
Shen, Y., Hu, J., Chen, Y., Liu, W., Li, Y., Yan, L., Xie, C., Zhang, W., Yu, M., Liu, W., 2020. Levodopa changes functional connectivity patterns in subregions of the primary motor cortex in patients with Parkinson's disease. Front. Neurosci. 14 https://doi.org/10.3389/fnins.2020.00647.
Shine, J. M. *et al.* Dopamine depletion alters macroscopic network dynamics in Parkinson's disease. *Brain* **142**, 1024-1034, doi:10.1093/brain/awz034 (2019).
Wang, J., Wang, X., Xia, M., Liao, X., Evans, A., He, Y., 2015. GRETNA: a graph theoretical network analysis toolbox for imaging connectomics. Front. Hum. Neurosci. 9 https://doi.org/10.3389/fnhum.2015.00386.
Wang, J., Li, Y., Huang, Z., Wan, W., Zhang, Y., Wang, C., Cheng, X., Ye, F., Liu, K., Fei, G., Zeng, M., Jin, L., 2018. Neuromelanin-sensitive magnetic resonance imaging features of the substantia nigra and locus coeruleus in de novo Parkinson's disease and its phenotypes. Eur. J. Neurol. 25 (7), 949–e73. https://doi.org/10.1111/ene.13628.
Watanabe, T., Wang, X., Tan, Z. & Frahm, J. Magnetic resonance imaging of brain cell water. **9**, 5084, doi:10.1038/s41598-019-41587-2 (2019).
Watts, D.J., Strogatz, S.H., 1998. Collective dynamics of 'small-world' networks. Nature 393 (6684), 440–442. https://doi.org/10.1038/30918.
Xia, M., Wang, J., He, Y., Csermely, P., 2013. BrainNet Viewer: a network visualization tool for human brain connectomics. PLoS ONE 8 (7), e68910.
Yeung, P. Y., Wong, L. L., Chan, C. C., Leung, J. L. & Yung, C. Y. A validation study of the Hong Kong version of montreal cognitive assessment (HK-MoCA) in Chinese older adults in Hong Kong. *Hong Kong medical journal = Xianggang yi xue za zhi* **20**, 504-510, doi:10.12809/hkmj144219 (2014).
Zerbi, V. *et al.* Rapid Reconfiguration of the Functional Connectome after Chemogenetic Locus Coeruleus Activation. *Neuron* **103**, 702-718 e705, doi:10.1016/j.neuron.2019.05.034 (2019).
Zhang, S., Hu, S., Chao, H. H. & Li, C. S. Resting-state functional connectivity of the locus coeruleus in humans: In Comparison with the Ventral Tegmental Area/Substantia Nigra Pars Compacta and the Effects of Age. *Cerebral cortex (New York, N.Y.: 1991)* **26**, 3413-3427, doi:10.1093/cercor/bhv172 (2016).
Zhou, C. *et al.* Progressive brain atrophy in Parkinson's disease patients who convert to mild cognitive impairment. **26**, 117-125, doi:10.1111/cns.13188 (2020).
Zhou, C., Gao, T., Guo, T., Wu, J., Guan, X., Zhou, W., Huang, P., Xuan, M., Gu, Q., Xu, X., Xia, S., Kong, D., Wu, J., Zhang, M., 2020. Structural covariance network disruption and functional compensation in Parkinson's disease. Front. Aging Neurosci. 12 https://doi.org/10.3389/fnagi.2020.00199.
Zhou, C., Guo, T., Wu, J., Wang, L., Bai, X., Gao, T., Guan, X., Gu, L., Huang, P., Xuan, M., Gu, Q., Xu, X., Zhang, B., Cheng, W., Feng, J., Zhang, M., 2021. Locus Coeruleus degeneration correlated with levodopa resistance in Parkinson's disease: a retrospective analysis. J. Parkinson's Dis. 11 (4), 1631–1640. https://doi.org/10.3233/JPD-212720.